



## Tracing impact of El Niño Southern Oscillation on coastal hydrology using coral $^{87}\text{Sr}/^{86}\text{Sr}$ record from Lakshadweep, South-Eastern Arabian Sea

Waliur Rahaman <sup>a,\*</sup>, Mohd Tarique <sup>a</sup>, A.A. Fousiya <sup>b</sup>, Priyesh Prabhat <sup>a,c</sup>, Hema Achyuthan <sup>d</sup>

<sup>a</sup> National Centre for Polar and Ocean Research, Ministry of Earth Sciences, Goa, India

<sup>b</sup> Department of Earth Sciences, Indian Institute of Technology, Kharagpur, India

<sup>c</sup> School of Earth, Ocean and Atmospheric Sciences, Goa University, Goa, India

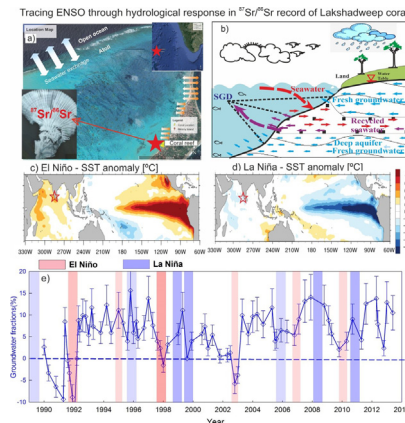
<sup>d</sup> Institute of Ocean Management, Anna University, Chennai, India



### HIGHLIGHTS

### GRAPHICAL ABSTRACT

- A novel approach to reconstruct past ENSO events using coral Sr isotope record from the Lakshadweep, Arabian Sea.
- Impact of ENSO events on coastal hydrology was traced through the reconstruction of past SGD using coral  $^{87}\text{Sr}/^{86}\text{Sr}$  record.
- This study reveals large supply of SGD up to ~20% due to higher rainfall during La Niña years compared to El Niño.



### ARTICLE INFO

Editor: Christian Herrera

#### Keywords:

$^{87}\text{Sr}/^{86}\text{Sr}$   
Arabian Sea  
ENSO  
Lakshadweep  
Corals  
SGD

### ABSTRACT

El Niño Southern Oscillation (ENSO) is one of the dominant climate modes influencing global precipitation and temperature. ENSO has a large impact on the monsoonal precipitations over the Indian subcontinent and thereby influences hydrological conditions. Due to dearth of long-term instrumental records of the hydrological parameters on sufficient spatial resolution, it is difficult to assess the impact of ENSO on regional hydrology. Though several geochemical proxies have been used to reconstruct past ENSO events through tracing the changes in past hydrological and climatic parameters, however, such reconstructions are often complicated by the influence of multiple processes and/or factors and their nonlinear relation with the proxy records. In this study, Sr isotope composition ( $^{87}\text{Sr}/^{86}\text{Sr}$ ) was measured in *Porites* coral from the Lakshadweep, south-eastern Arabian Sea to reconstruct past ENSO events and to trace its regional hydrological impacts. The high precision measurements of  $^{87}\text{Sr}/^{86}\text{Sr}$  in Lakshadweep coral show resolvable variations ranging from 0.709080 to 0.709210. The  $^{87}\text{Sr}/^{86}\text{Sr}$  record shows an inverse relation with Niño 3.4 record; lower values matched with El Niño years and higher values with La Niña years. Our investigation reveals that ENSO driven precipitation changes impacted submarine groundwater discharge (SGD) to the Minicoy Atoll and resulted in  $^{87}\text{Sr}/^{86}\text{Sr}$  variations of the Minicoy Atoll water. Therefore, deviation from the average seawater  $^{87}\text{Sr}/^{86}\text{Sr}$  value can be quantified in terms of SGD contribution to the Minicoy Atoll. Our estimates based on binary mixing between seawater and SGD  $^{87}\text{Sr}/^{86}\text{Sr}$  suggest a significant supply of SGD, maximum up to ~20 % of the total volume of the Minicoy Atoll during La Niña years due to higher rainfall compared to El Niño years. This finding

\* Corresponding author.

E-mail address: [waliur@ncpor.res.in](mailto:waliur@ncpor.res.in) (W. Rahaman).

highlights potential application of coral  $^{87}\text{Sr}/^{86}\text{Sr}$  record as an alternate proxy to reconstruct past ENSO events and to trace its quantitative impact on regional hydrology, chemical and nutrient fluxes to coastal oceans via SGD.

## 1. Introduction

The El Niño–Southern Oscillation (ENSO) is a dominant climate mode that originates in the tropical eastern Pacific Ocean and influences global climate through the modulation of global temperature and precipitations with recurrence intervals of 2–7 years. ENSO has three distinct phases i.e. Neutral, La Niña and El Niño; the La Niña and El Niño are opposite phases that cause high and low rainfall over India respectively (Azad and Rajeevan, 2016; Kripalani and Kulkarni, 1997; Rajeevan and Pai, 2007). The impact of ENSO events on the regional hydrological conditions is difficult to assess due to the dearth of long-term continuous records of hydrological and meteorological parameters at sufficient spatio-temporal resolutions. To reconstruct past ENSO events and understand its regional hydrological impacts during the pre-instrumental era, we have to depend on either global climate models or proxy-based reconstructions such as oxygen isotope records from tropical corals (Ahmad et al., 2011; Chakraborty et al., 2012; Corrège, 2006; Liu et al., 2014; Sadler et al., 2014; Thompson, 2022), tree rings (D'Arrigo et al., 2005), cave carbonates (stalagmites) (Consortium, 2017) and Antarctic ice cores (Rahaman et al., 2019). In addition, a few indirect proxy records such as sedimentation records from the Amazon floodplain (Aalto et al., 2003) and Sr, Nd isotope compositions of sediment core records from the Tumbes River basin in Peru (Moquet et al., 2020) were also used to infer about past ENSO events and its impact on regional climate and sediment dynamics. The model-based simulations of ENSO are generally associated with large uncertainties and often show diverging results (Cai et al., 2014; Collins et al., 2010). Several marine and terrestrial proxy records have been employed to reconstruct ENSO-driven precipitation changes; however, such attempts are often hindered by a dearth of continuous high-resolution records and nonlinear response of proxies to precipitation changes. Coral is an excellent archive that provides high-resolution proxy records comparable to instrumental resolution and can go much beyond the instrumental era. Trace element ratios measured in corals such as Sr/Ca, Li/Mg, and Mg/Ca have been extensively used as a proxy for past sea surface temperature (SST) and also to infer about the past ENSO activity (DeLong et al., 2013; Raddatz et al., 2013; Sagar et al., 2015). Proxy derived SST records of Lakshadweep coral reefs reveal the dominant influence of ENSO on SST variability (Sagar et al., 2015). However, only few attempts have been made so far to reconstruct past precipitation changes induced by ENSO events and its impact on regional climatic and hydrological conditions (Aalto et al., 2003; Braganza et al., 2009; Fowler et al., 2012; Moquet et al., 2020). Further, these proxy records do not provide detailed information about the past hydrological changes such as precipitations, continental runoff, salinity, and coastal upwelling. Oxygen isotope ( $\delta^{18}\text{O}$ ) measured in corals has been extensively used as a proxy to reconstruct past sea surface salinity (SSS) and to infer about the past precipitation changes (Pfeiffer et al., 2019; Zinke et al., 2021). However, seawater  $\delta^{18}\text{O}$  is known to be influenced by both temperature and salinity, it is difficult to deconvolute the signal of past SSS and to infer about the past precipitation changes (Achyuthan et al., 2013). Further, SSS can be influenced by the changes in upwelling intensity, circulation, continental runoff, and submarine groundwater discharge (SGD), therefore, it is difficult to disentangle the contributions from precipitation changes. Given these caveats attached and uncertainties associated with the applications of these proxies, it is imperative to explore alternate proxies to trace the impact of ENSO events on precipitation and other hydrological parameters. Radiogenic isotopes of Sr ( $^{87}\text{Sr}/^{86}\text{Sr}$ ) measured in corals could be a promising proxy because of distinct signatures of the various hydrological components/sources i.e. seawater, groundwater, rainfall, continental runoff and river discharge and hence could be used to elucidate past changes in the regional hydrological conditions impacted by ENSO events.

In the present study, we have measured  $^{87}\text{Sr}/^{86}\text{Sr}$  ratio in the Lakshadweep coral (*Porites*) and generated a high resolution record at sub-annual scales from 1990 to 2013. These coral samples have already been studied for stable carbon ( $\delta^{13}\text{C}$ ) and oxygen isotopes ( $\delta^{18}\text{O}$ ) to investigate its potential application as a proxy for southwest monsoonal variability (Fousiya et al., 2016; Tarique et al., 2021) and boron isotope ( $\delta^{11}\text{B}$ ) as a proxy for the reconstruction of Arabian Sea surface ocean pH variability and ocean acidification trend (Tarique et al., 2021). In addition, high resolution records of Sr/Ca and Li/Mg ratios were also obtained by Tarique et al. (2021) from the same coral samples to improve the chronology of this coral. In this study, Sr isotopes were analysed in the same aliquots of coral samples in which  $\delta^{11}\text{B}$  and trace element concentrations were measured. The high resolution coral  $^{87}\text{Sr}/^{86}\text{Sr}$  record in the present study together with published records of elemental ratios (Sr/Ca and Li/Mg) and  $\delta^{18}\text{O}$  were used to reconstruct past ENSO events and to trace its impact on regional hydrological conditions.

## 2. Material and methods

### 2.1. Geography, climate and hydrogeological settings of the Minicoy

The Minicoy Island, Lakshadweep archipelago is located in the south-eastern Arabian Sea (Fig. 1) which is one of the world's largest atoll reef systems comprised of several atolls formed above the submerged Lakshadweep–Chagos volcanic ridges (Wilkinson, 2000). The Minicoy Atoll is located at a distance of ~400 km off Kochi (south-west coast of India) with lagoon area of ~31 km<sup>2</sup> (Fig. 1) and a water depth of up to 10 m (Mallik, 2017; Pillai, 1971). The ridge rises from the deep sea and is composed of basalts, which is capped by recent coral reefs in the form of atoll and coral banks.

The south-eastern Arabian Sea is characterised by seasonal reversal of surface currents caused by the reversal of winds (Shankar et al., 2002). The sea level and thermocline of the Lakshadweep region undergo large seasonal changes due to the reversal of wind. This seasonal wind reversal results in prominent seasonal cycles of SST ranging from >30 °C during April–May to <27 °C during August–September (Boyer et al., 2019). The maximum temperature is observed in the months of April and May (29° to 31 °C) and minimum during the months of December and January (27 °C and 29 °C) (Boyer et al., 2019). Sea surface salinity (SSS) of this region is mainly controlled by evaporation-precipitation balance and freshwater runoff (Behara et al., 2019; Shankar et al., 2002). The southwest coast of India, including the Lakshadweep region receives the highest rainfall during summer monsoon (May–September) with an average annual rainfall on the island of about 1640 mm (Md and Vinayachandran, 2013). However, the annual rainfall of this region is affected by the ENSO events; high rainfall (above normal) occurs during the La Niña years due to intensified monsoon and opposite during the El Niño years (Rajeevan et al., 2008). The ERA 5 reanalysis precipitation record (1979–2019) regressed with the Nino 3.4 and southern oscillation index (SOI) records highlight the regions which are significantly (at 90 % significance level) impacted by the ENSO events. Our study region shows a significant positive correlation (at 90 % significance level) with the SOI record (Supplementary Fig. S1) and thus clearly indicates that precipitation over this region is influenced by ENSO events.

Though the Minicoy Island receives high rainfall, this region has limited surface water and groundwater storage with sporadic occurrences of small lenses of floating freshwater over saltwater. High porosity of the aquifers allows infiltration of freshwater and mixes with seawater. The rainfall infiltrates into the ground and a small portion of it goes to recharge the groundwater and the majority of it is lost as a subsurface runoff and evaporation.

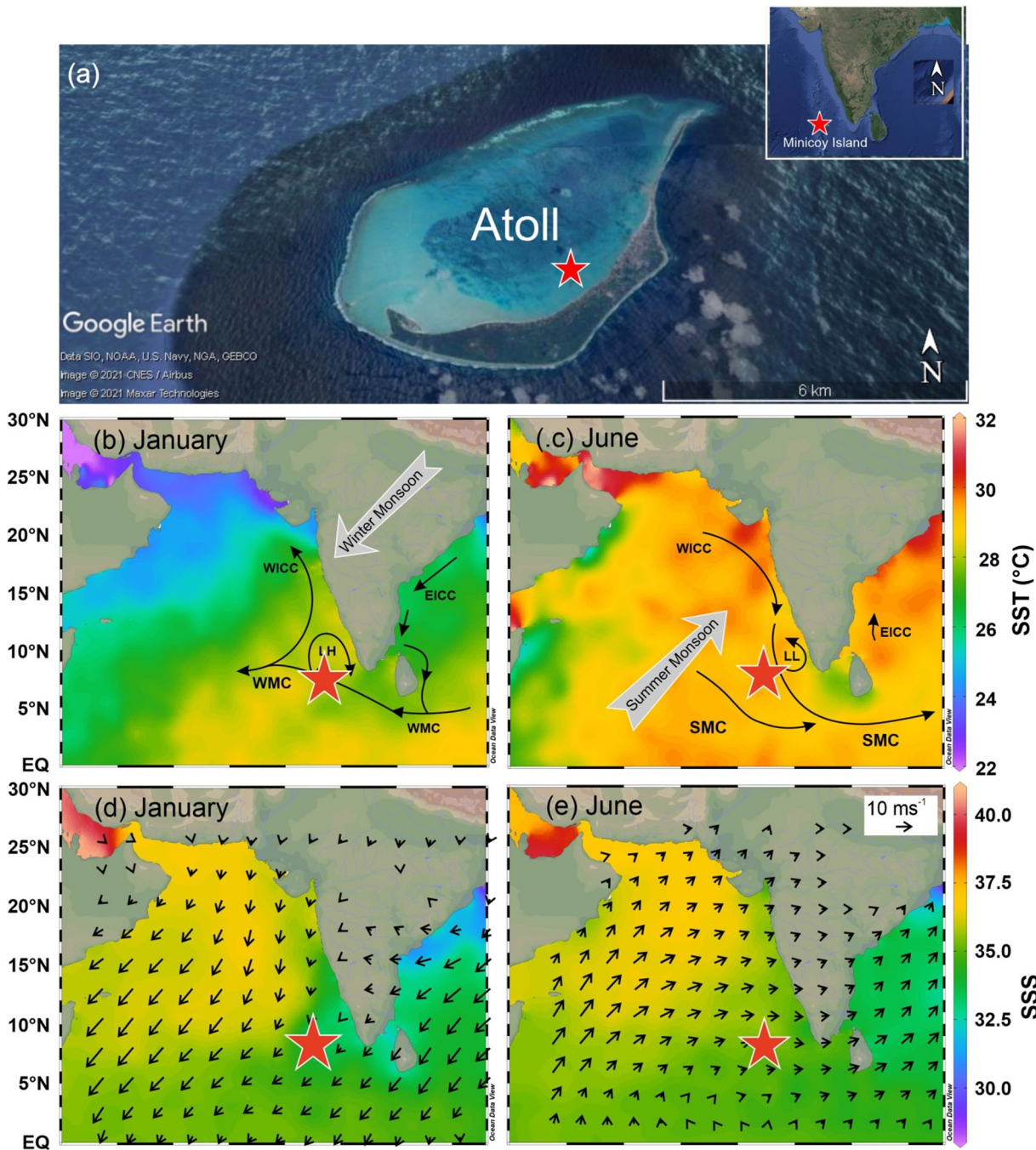


**Fig. 1.** Oceanographic and hydrographic settings of the study area. (a) Google earth view of Minicoy Island with the location of the sampling site (red star). In panels (b) to (e), colour map represents the climatological mean of SST and SSS of the Arabian Sea for January and June (World Ocean Atlas 2018) (Boyer et al., 2019). Arrows represent the surface water currents (Schott et al., 2009; Shankar et al., 2002); WMC—Winter Monsoon Current, SMC—Summer Monsoon Current, EICC—East India Coastal Current, WICC—West India Coastal Current, LH—Lakshadweep High, LL—Lakshadweep Low. The vector arrows in panel (d) and (e) represent the climatological mean wind direction and length of the arrow represents the magnitude of wind speed (Kalnay et al., 1996). The blue star represents location of the coral sample used in this study.

The position and thickness of the interface/interface zone between fresh and saline water are largely controlled by diurnal tidal fluctuation, seasonal water level fluctuation, and groundwater recharge (Md and Vinayachandran, 2013).

## 2.2. Coral sample collection, subsampling and its cleaning procedure

This coral sample was collected from the remote and undisturbed area in the Lakshadweep where the impact of anthropogenic activities is minimal. Details of the coral sampling have been discussed elsewhere

(Fousiya et al., 2016; Tarique et al., 2021). Briefly, a specimen of massive *Porites lutea* coral was collected live on 21st October 2013 during low tide from the Minicoy Island, Lakshadweep ( $8^{\circ}16'55.2''N$ ,  $73^{\circ}03'16.8''E$ , 2 m water depth) in the south-eastern Arabian Sea. After the sample collection, the coral sample was soaked in 5%  $H_2O_2$  for 2 h to remove the organic matter and subsequently rinsed with MilliQ water multiple times. A ~7 mm-thick slab was cut along the maximum growth axis of the coral with a diamond blade for subsampling. The slab was cleaned with MilliQ water and ultrasonicated for 30 min followed by soaking in 5% sodium hypochlorite (NaOCl) solution for 12 h. Finally, the sample (coral slab) was rinsed

three times with MilliQ water in an ultrasonic bath and then dried in a hot air oven at 60 °C. To identify the annual density bands, X-ray photography of the sample was done at the SMRC Hospital, Goa using a Siemens Heliophos D® machine. The X-ray image was used as a frame of reference for continuous sub-sampling along the maximum growth axis (supplementary Fig. S2). Sub-sampling was done using a low-speed handheld drill and slab was drilled along a line to get the samples. For each sample, length of the line was ~2–3 mm, and sampling depth and width were around 1–2 mm yielding an average of 3–4 samples per year. About 10–20 mg of the drilled material was collected for each sample for geochemical analysis.

Few groundwater ( $n = 3$ ) samples were also collected from the close proximity to the coral reef. These samples were filtered onsite through 0.4 µm cellulose acetate filters immediately after the sample collection and acidified to pH ~2 using ultra-pure HNO<sub>3</sub>. These samples were stored in pre-cleaned high-density polypropylene bottles for Sr isotope analysis in the laboratory.

### 2.3. Sr isotope measurements in coral and water samples

About 3 to 5 mg of CaCO<sub>3</sub> per sample were taken for the trace elements and the Sr isotope analysis. The samples were cleaned following the protocol adapted from Barker et al. (2003). Briefly, the powdered samples were thoroughly rinsed multiple times with MilliQ water and methanol with 30 s of ultra-sonication to remove the clay. Subsequently, residual organic matter was removed by treating with NaOH-H<sub>2</sub>O<sub>2</sub> buffer (0.2 M NaOH in 1% H<sub>2</sub>O<sub>2</sub>) in an ultrasonic bath followed by rinsing with MilliQ. Any secondary chemisorbed elements on the surface of aragonite were removed by treating twice with extremely low strength ultra-clean 0.001 M HCl and 30 s of ultrasonication. Chemically cleaned samples were dissolved in 70 µl of 1 M HCl (Fisher Scientific Optima® grade). An aliquot of 20 µl dissolved samples were taken and dried completely. The dried samples were further treated with a few drops of HNO<sub>3</sub> to convert the medium and then dried completely. The dried samples were taken in 3 N HNO<sub>3</sub> matrix in 1 ml volume for column chromatography. Sr was separated using Eichrom® Sr specific resin (50–100 µm) (Rahaman and Singh, 2012). In addition, seawater samples ( $n = 3$ ) and groundwater samples ( $n = 3$ ) collected from the Lakshadweep region were also analysed for the Sr isotope compositions (Table 1). The procedure for the extraction of Sr from water samples and its isotopic composition measurements were adopted from earlier studies (Rahaman and Singh, 2012; Rahaman et al., 2011). About 0.5 to 1 g of filtered and acidified water samples were taken for Sr isotope analysis. These samples were taken into Teflon vials and dried completely on a hotplate. These dried samples were treated with few drops of concentrated HNO<sub>3</sub> to remove organic matter and dried completely. Finally re-dissolved in 1 ml 3 N HNO<sub>3</sub> for the column chromatography. Then Sr was extracted and purified using Eichrom® Sr-Spec resin (50–100 µm) following the established procedure (Nuruzzama et al., 2020; Pin and Bassin, 1992; Rahaman and Singh, 2012). To check the quality of the analysis, international seawater reference standard NASS 6 was also processed along with the samples following the same procedure. In addition, a few blanks were also processed in each batch of samples following the same procedure. All the samples and standards were prepared under the class 100 laminar flow inside a class 10,000 metal-free clean laboratory.

Sr isotopes were measured in filtered and acidified water samples using the multi-collector ICPMS (Neptune Plus; Thermo Scientific) facility at NCPOR, Goa, India. The Sr isotope analyses were performed following the established analytical protocol discussed elsewhere (Nuruzzama et al., 2020; Rahaman and Singh, 2012). For instrumental mass bias corrections, the measured <sup>86</sup>Sr/<sup>88</sup>Sr ratio was normalized to its natural value of 0.1194. A standard solution of NIST NBS-987 was measured at an interval of every five samples during analysis. The average <sup>87</sup>Sr/<sup>86</sup>Sr value of NBS-987 during the course of analysis yielded a value of 0.710239 ± 0.000026 (2 $\sigma$ ,  $n = 22$ ) which is well within the reported range (0.710250 ± 0.000040 [2 $\sigma$ ]) (Weis et al., 2006). The international seawater standard, NASS6 measured along with the water samples yielded an average value of 0.709160 ± 0.000010 (2 $\sigma$ ,  $n = 4$ ) which is identical to the

reported value 0.709170 (Wakaki et al., 2017). The Sr isotopic data are reported after sample-standard bracketing normalization following the approach of Weis et al. (2006). The total procedural blank determined for Sr was 430 pg, <0.04 % of total Sr (~1 µg) typically analysed in samples and hence, blank correction was not done.

### 2.4. Chronology of the coral

The age model of the coral was established by Fousiya et al. (2016) based on the identification of the annual density band in X-ray radiography of the coral and seasonality in the δ<sup>18</sup>O record. However, due to missing layer(s) and/or occurrence of multiple layer(s) in a year might lead to erroneous counting and large uncertainty in the age model. Further, seasonal signal in δ<sup>18</sup>O record is often complicated by combined influences of salinity and temperature. To circumvent this problem, Sr/Ca ratio in corals has been a robust proxy for SST (DeLong et al., 2007; Fowell et al., 2016; Leupold et al., 2021; Pfeiffer et al., 2009; Sagar et al., 2016). In order to improve the previous chronology established by Fousiya et al. (2016), high resolution measurements of trace elements were performed in the subsequent study (Tarique et al., 2021) to obtain Sr/Ca and Li/Mg ratios from the same samples. Based on the revised chronology, the coral record represents ~23 years of growth record starting from the year 1990 and ending in the year 2013. The uncertainty in the age model is ~3–4 months for any calendar year. Details of the revised chronology have been discussed elsewhere (Tarique et al., 2021). It is important to mention here that with this uncertainty in the revised age model, we could resolve interannual variability in the <sup>87</sup>Sr/<sup>86</sup>Sr record with high confidence.

### 2.5. Estimation of salinity

The δ<sup>18</sup>O of coral carbonate skeleton reflects both seawater temperature and seawater δ<sup>18</sup>O (Correge, 2006; Hendy et al., 2002; McCulloch et al., 1994). Combining with Sr/Ca record in the skeleton, the thermal and hydrological conditions that are recorded in δ<sup>18</sup>O can be decoupled (Gagan et al., 1998; McCulloch et al., 1994; Shen et al., 2005). After removing temperature effect, δ<sup>18</sup>O of the seawater was calculated following the equation taken from Chakraborty and Ramesh (1993). The following equation is valid within the SST and salinity range 26.8 to 29.8 °C and 33 to 36 respectively.

$$\delta_{sw} = \left( \frac{T - 3}{4.68} \right) + \delta_{coral} \quad (i)$$

Further, based on the salinity-δ<sup>18</sup>O relation established for the surface (0–50 m water depth) water in the south-eastern Arabian Sea Singh et al. (2010), past sea surface salinity can be reconstructed using the coral δ<sup>18</sup>O records. The following regression equation was used to reconstruct the salinity

$$SSS = 0.5972 \delta_{sw} + 34.982 \quad (ii)$$

The estimate of the past SSS using the above equation assumes a constant temporal δ<sup>18</sup>O-SSS relation observed at a given time.

## 3. Results

The <sup>87</sup>Sr/<sup>86</sup>Sr ratio of the Lakshadweep coral ranges from 0.70908 ± 0.000010 to 0.70921 ± 0.000012 (2 $\sigma$ ) ( $n = 78$ ) (Fig. 2a; Table 1) which are distinct from the average Arabian Sea water value 0.709150 ± 0.000004 (2 $\sigma$ ) (Rai, 2008). Further, we have measured the seawater reference standard NASS-6 (0.709160 ± 0.000006 (2 $\sigma$ ,  $n = 4$ )), which is similar to the reported value of the Arabian Sea (Rai, 2008). Few groundwater samples collected from the Lakshadweep measured in the present study show a narrow range with an average of 0.709210 ± 0.000010 (2 $\sigma$ ,  $n = 3$ ). This indicates that the groundwater is more radiogenic compared to the Arabian Seawater. The observed ranges in the coral <sup>87</sup>Sr/<sup>86</sup>Sr

**Table 1**

Sr isotope data of coral, groundwater, and seawater standard NASS-6.

Age (year A.D)	$^{87}\text{Sr}/^{86}\text{Sr}$	Error ( $1\sigma$ )
Coral samples		
1990.0	0.709160	0.000005
1990.3	0.709137	0.000006
1990.8	0.709124	0.000006
1991.3	0.709112	0.000006
<b>1991.3 R</b>	<b>0.709108</b>	<b>0.000005</b>
1991.4	0.709181	0.000006
1991.6	0.709148	0.000006
1991.7	0.709137	0.000008
1991.9	0.709114	0.000009
1992.0	0.709079	0.000006
<b>1992.0 R</b>	<b>0.709075</b>	<b>0.000006</b>
1992.2	0.709150	0.000007
1992.3	0.709182	0.000006
<b>1992.3 R</b>	<b>0.709177</b>	<b>0.000005</b>
1992.4	0.709174	0.000006
1992.6	0.709186	0.000008
1992.8	0.709185	0.000006
1993.0	0.709170	0.000007
1993.2	0.709192	0.000007
1993.3	0.709177	0.000007
1993.8	0.709172	0.000006
1994.2	0.709194	0.000006
1994.5	0.709172	0.000007
1995.0	0.709190	0.000007
1995.3	0.709180	0.000007
1995.6	0.709165	0.000006
1995.8	0.709205	0.000006
1996.0	0.709172	0.000006
<b>1996.0 R</b>	<b>0.709166</b>	<b>0.000004</b>
1996.2	0.709181	0.000006
1996.3	0.709167	0.000006
1996.7	0.709176	0.000007
1997.0	0.709199	0.000005
1997.3	0.709178	0.000006
1997.6	0.709165	0.000004
1997.8	0.709159	0.000005
1998.0	0.709144	0.000004
1998.3	0.709162	0.000004
1999.0	0.709171	0.000005
1999.3	0.709190	0.000007
1999.6	0.709182	0.000006
1999.9	0.709165	0.000006
<b>1999.9 R</b>	<b>0.709155</b>	<b>0.000005</b>
2000.6	0.709171	0.000006
2000.8	0.709177	0.000007
2001.0	0.709159	0.000006
2001.3	0.709170	0.000007
2001.8	0.709152	0.000007
2002.3	0.709153	0.000008
2002.5	0.709155	0.000006
2002.8	0.709127	0.000006
2003.0	0.709135	0.000008
2003.3	0.709186	0.000007
2003.7	0.709171	0.000006
2004.0	0.709185	0.000006
2004.3	0.709187	0.000007
2004.7	0.709179	0.000006
2005.3	0.709192	0.000005
2005.5	0.709165	0.000006
2005.6	0.709167	0.000007
2005.9	0.709174	0.000007
2006.3	0.709173	0.000005
2006.8	0.709170	0.000007
2007.1	0.709183	0.000006
2007.5	0.709197	0.000006
2007.9	0.709200	0.000006
2008.8	0.709194	0.000006
2009.1	0.709182	0.000006
2009.3	0.709171	0.000005
2009.8	0.709158	0.000007
2010.3	0.709165	0.000006
2010.7	0.709183	0.000005
2011.3	0.709166	0.000004
<b>2011.3 R</b>	<b>0.709157</b>	<b>0.000005</b>

**Table 1 (continued)**

Age (year A.D)	$^{87}\text{Sr}/^{86}\text{Sr}$	Error ( $1\sigma$ )
2011.6	0.709195	0.000006
2012.3	0.709199	0.000006
2012.4	0.709179	0.000008
<b>2012.4 R</b>	<b>0.709171</b>	<b>0.000004</b>
2012.8	0.709159	0.000008
2013.0	0.709196	0.000006
2013.4	0.709188	0.000006
Groundwater		
GW1	0.70920	0.000006
GW2	0.70922	0.000005
<b>GW2 R</b>	<b>0.70920</b>	<b>0.000005</b>
GW3	0.70919	0.000005
<b>GW3 R</b>	<b>0.70921</b>	<b>0.000005</b>
Seawater standard NASS6		
NASS6-2	0.709163	0.000005
NASS6-3	0.709149	0.000004
NASS6-4	0.709157	0.000005
NASS6-5	0.709163	0.000005

R-replicates.

are higher than the analytical uncertainty of  $\pm 10$  ppm ( $2\sigma$ ) and hence the natural variations can be resolved. The sub-annually resolved coral based seawater  $^{87}\text{Sr}/^{86}\text{Sr}$  from the Lakshadweep region clearly indicates significant inter-annual variations (Fig. 2). We have compared  $^{87}\text{Sr}/^{86}\text{Sr}$  record with the published records of  $\delta^{18}\text{O}$  and elemental ratios of Sr/Ca and Li/Mg measured in the same samples (Tarique et al., 2021). The excursions observed in these proxy records show good correspondence (Fig. 3). The  $^{87}\text{Sr}/^{86}\text{Sr}$  profile shows an opposite trend with the  $\delta^{18}\text{O}$  record and significant inverse relation with a lag of about six months (Fig. 3b). In previous study, Tarique et al. (2021) have demonstrated an inverse relationship between Sr/Ca ( $r = 0.54, n = 79, p < 0.01$ ) and Li/Mg ( $r = 0.38, n = 79, p < 0.01$ ) with the SST record (HadISST). Power spectrum analyses of the Li/Mg record revealed a significant (at 95 %  $\chi^2$  level) periodicity of 7.8 years and strongly coeval with the ENSO (SOI) record (Tarique et al., 2021).

The past salinity reconstructed based on the  $\delta^{18}\text{O}$  record and SST ranges from 34.6 to 36.2 °C with an average of 35.6 °C which is consistent with the previous report (Boyer et al., 2019). The reconstructed salinity closely follows the  $^{87}\text{Sr}/^{86}\text{Sr}$  profile; excursions of less radiogenic values coincide with the higher salinity. The higher salinity and less radiogenic Sr isotope matched well with the El Niño years (Fig. 4a, b). The higher values of Niño 3.4 (El Niño periods) coincide with the lower value of  $^{87}\text{Sr}/^{86}\text{Sr}$ , similar to that of average seawater value whereas higher  $^{87}\text{Sr}/^{86}\text{Sr}$  values were observed during the lower Niño 3.4 (La Niña) periods; they show significant inverse correlation ( $r = 0.49, p < 0.01, n = 75$ ) (Fig. 4a). Overall, our multi-proxy records including the coral  $^{87}\text{Sr}/^{86}\text{Sr}$  record show good correspondence with the ENSO index (SOI) and Niño 3.4 record (Fig. 4).

#### 4. Discussion

Our reconstructed salinity record shows a good correspondence with the Niño 3.4 record; salinity peaks match well with the El Niño and dips with the La Niña years (Fig. 4b). This indicates effect of ENSO on the monsoonal precipitations which influences salinity of the Minicoy Atoll; higher precipitation during the La Niña years caused more dilution of seawater and lowered the salinity whereas opposite happened during the El Niño years due to weaker monsoon with lower precipitation and higher evaporation (Supplementary Fig. S1). Recent studies have demonstrated that monsoon runoff is capable of changing the  $\delta^{18}\text{O}$ -Salinity relation in the northern Indian Ocean (Ahmad et al., 2011; Singh et al., 2010). The  $\delta^{18}\text{O}$ -depleted runoff has resulted from higher rainfall with lower  $\delta^{18}\text{O}$  commonly referred as ‘amount effect’ (Dansgaard, 1964). Thus, the depleted  $\delta^{18}\text{O}$  values in the  $\delta^{18}\text{O}$ -salinity record indicate stronger monsoon rainfall whereas enriched values indicate less rainfall/or drought conditions (Supplementary Fig. S3). The  $\delta^{18}\text{O}$  values in the Minicoy Atoll is controlled by multiple processes/factors such as mixing, evaporation,

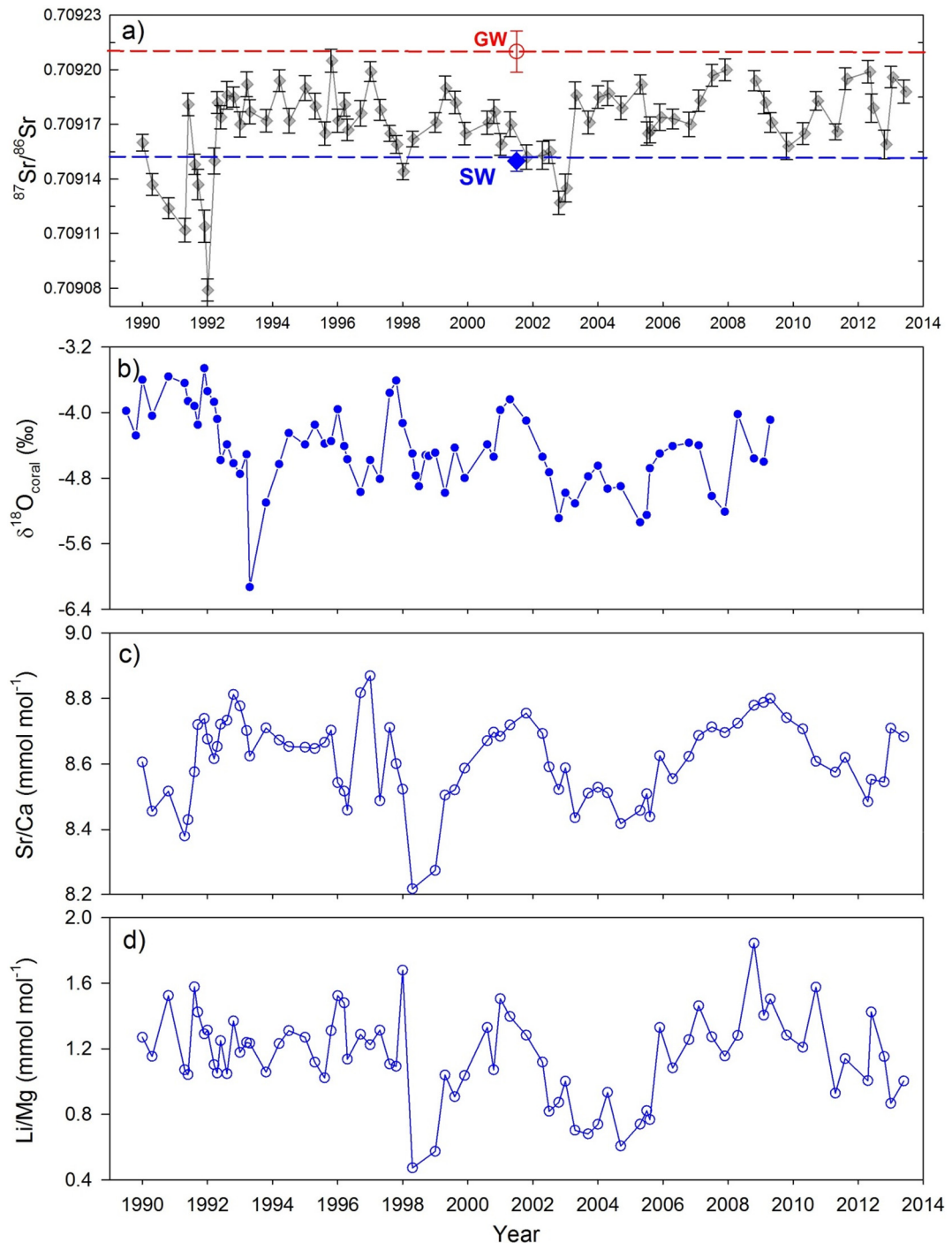


**Fig. 2.** Comparison of multiple proxy records of the Lakshadweep coral. (a) Coral  $^{87}\text{Sr}/^{86}\text{Sr}$  record in the present study is compared with previously published records of (b)  $\delta^{18}\text{O}$  and (c, d) elemental ratios of Sr/Ca and Li/Mg measured in the same samples (Tarique et al., 2021). Red and blue coloured dashed lines indicate average groundwater (GW) and seawater (SW) values.

precipitation and upwelling and therefore becomes difficult to quantify the changes in hydrological conditions based on the coral  $\delta^{18}\text{O}$  record. Whereas Sr isotope behaves as a conservative tracer and does not get affected by the above processes/factors (Fan et al., 2019) and hence the variability in the coral  $^{87}\text{Sr}/^{86}\text{Sr}$  record can only be explained in terms of mixing of various sources with distinct isotope signatures (Danish et al., 2020; Rahaman and Singh, 2012). However, few studies have reported thermal effect on Sr isotope composition ( $\delta^{88}/^{86}\text{Sr}$ ) measured in the cold-water corals (Fietzke and Eisenhauer, 2006; Rüggeberg et al., 2008). However, with the improvement in analytical method using recently developed double spike TIMS technique, the results of  $\delta^{88}/^{86}\text{Sr}$  in the same coral samples

differ from those obtained with less precise methods (Raddatz et al., 2013; Wei et al., 2022). They have demonstrated that  $\delta^{88}/^{86}\text{Sr}$  measured in scleractinian cold-water corals is not controlled by seawater temperature (Wei et al., 2022), rather reflects the Sr isotopic composition of seawater and may thus be useful to reconstruct Sr isotopic composition of the past seawater. Further, laboratory studies based on culture experiments of marine biogenic carbonates have demonstrated that under variable environmental conditions (e.g. seawater pH, temperature and salinity) chemical compositions might be affected but do not influence Sr isotope composition; they record the Sr isotope composition of ambient seawater (Liu et al., 2015). Therefore, the Lakshadweep coral growing in the Minicoy

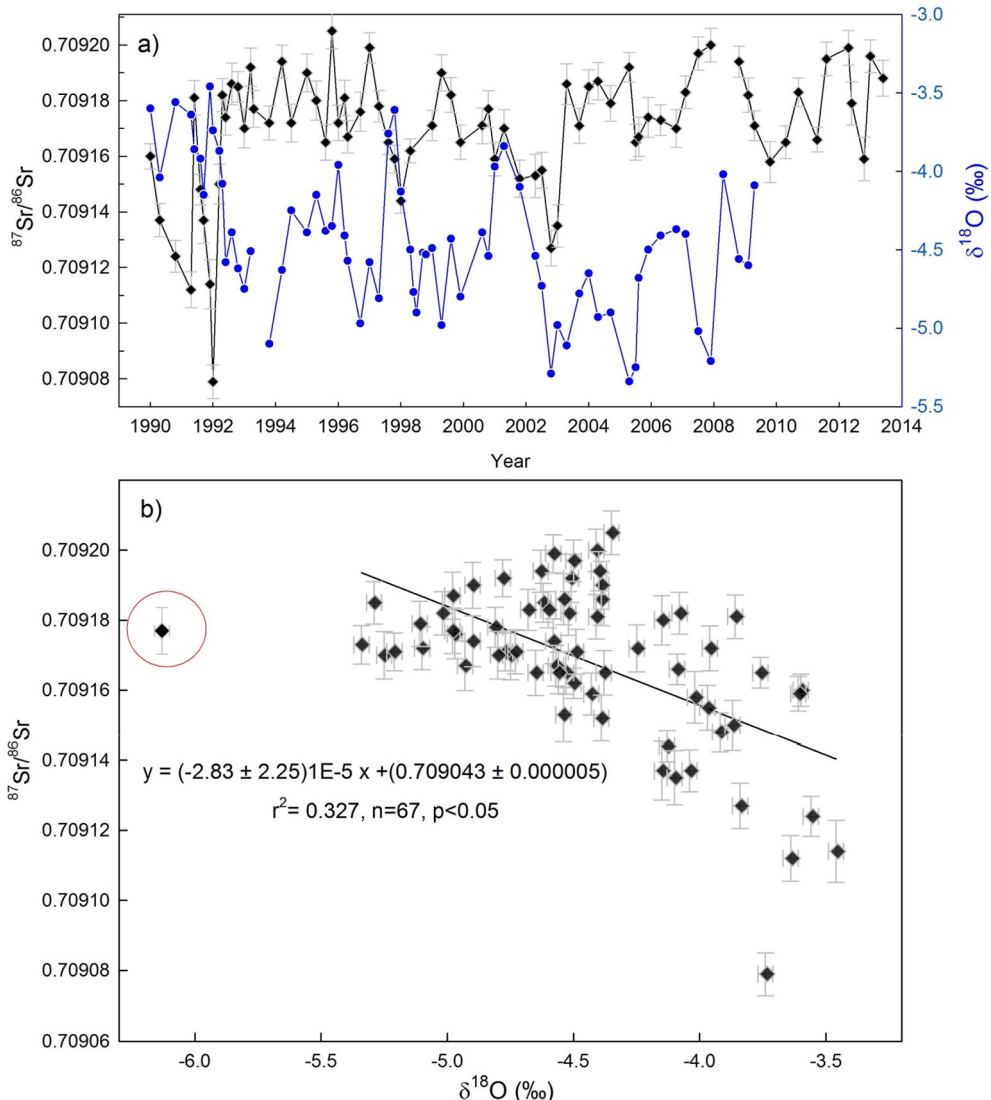


**Fig. 3.** (a) Comparison of coral  $^{87}\text{Sr}/^{86}\text{Sr}$  and  $\delta^{18}\text{O}$  profiles.  $^{87}\text{Sr}/^{86}\text{Sr}$  profile is plotted with a lag of about six months in the time series plot (a) and (b) correlation plot. The  $^{87}\text{Sr}/^{86}\text{Sr}$  shows significant inverse relation ( $r = 0.57$ ,  $n = 67$ ,  $p < 0.05$ ) with  $\delta^{18}\text{O}$  with a lag of about six months in the entire record (1990–2013). The data point shown in the red circle was not considered in the regression fit.

Atoll water will acquire its value of  $^{87}\text{Sr}/^{86}\text{Sr}$  from the water in which they grow and enable us to quantify the contribution from various sources, provided that the Sr isotope compositions of endmembers are well constrained (Figs. 5, 6d).

To explain the variability in coral  $^{87}\text{Sr}/^{86}\text{Sr}$  record, it is important to have knowledge of Sr sources and their isotope compositions. The primary sources of Sr in the Minicoy Atoll that control the dissolved Sr isotope budgets are seawater, SGD, rainwater and continental runoff either directly from the coastal region and/or via river discharge (Fig. 5). The Sr concentration measured in rainwater over north-western India ranges from 32 to 191 nM (Chatterjee and Singh, 2012), almost three orders of magnitude lower than Arabian seawater concentration 88  $\mu\text{mol/kg}$  (Rahaman and Singh, 2012) and therefore unlikely to alter Sr isotope composition of the Minicoy Atoll water. The Minicoy Island does not have any rivers or streams and therefore, any deviations from the modern seawater  $^{87}\text{Sr}/^{86}\text{Sr}$  value clearly indicate contributions of Sr via SGD and surface runoff. The Minicoy Atoll is far away from the west coast of India and hence influence of river discharge and surface runoff is minimal and/or negligible. Therefore, SGD is the most possible source that can contribute significantly to the Sr isotope budget of the Minicoy Atoll. As illustrated in Fig. 5, one side of

the Minicoy Atoll is connected to the open sea and exchanges water with the Atoll whereas the other side of the Atoll is enclosed by the island (Fig. 5). The SGD is supplied to the Minicoy Atoll either through seawater invasion into the coastal aquifer and recycled back and/or the fresh groundwater discharge from the island (Fig. 6d). An illustration in Fig. 5 clearly shows how Minicoy Atoll acts as a host for the mixing of only two components i.e. Arabian Sea water and SGD from the Minicoy Island and hence Sr isotope variation is primarily controlled by the contributions from these two sources.

SGD has been recognized as a potential source of dissolved elements including Sr to coastal oceans (Basu Asish et al., 2001; Huang et al., 2011; Johannesson et al., 2011; Moore, 2010a). Further, Rahaman et al. (2011) have reported that SGD is an important supplier of Sr to the west coast of India based on the study of dissolved Sr and  $^{87}\text{Sr}/^{86}\text{Sr}$  in the Narmada, Tapi, and the Mandovi estuaries from the west coast of India. This study has highlighted the importance of SGD fluxes in modifying the Sr isotope composition of coastal waters and provided estimates of SGD fluxes for the west coast of India; the SGD flow rate ranges between ~5 and 280 cm/day for the pre-monsoon and monsoon seasons which are consistent with those reported from the southwest coast of India using dissolved

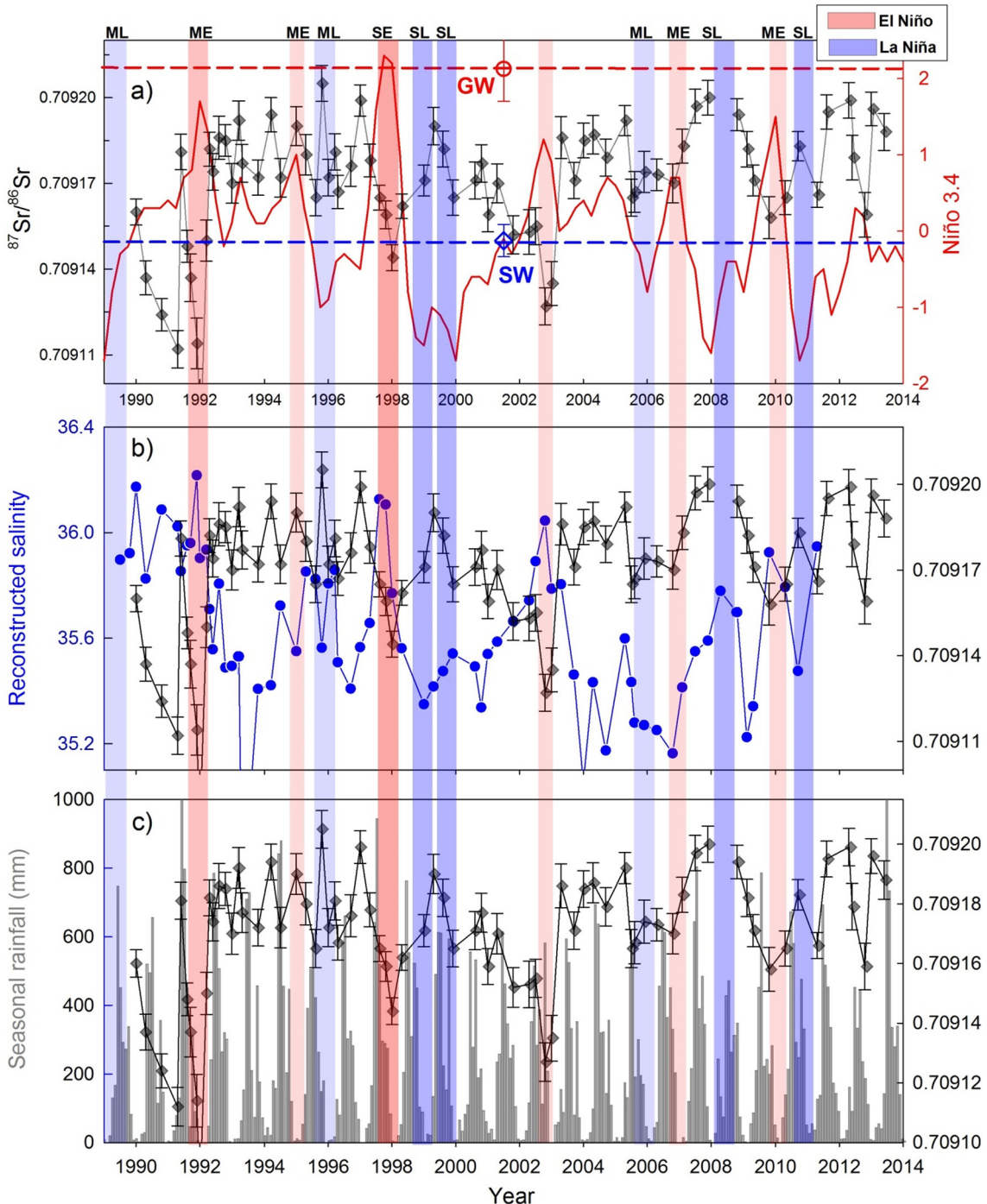


**Fig. 4.** Role of ENSO events (El Niño and La Niña) on past records of  $^{87}\text{Sr}/^{86}\text{Sr}$  variations in the Minicoy Atoll. (a) Coral  $^{87}\text{Sr}/^{86}\text{Sr}$  is compared with Niño 3.4 index taken from [https://psl.noaa.gov/gcos\\_wgsp/Timeseries/Nino34/](https://psl.noaa.gov/gcos_wgsp/Timeseries/Nino34/). The higher values of Niño 3.4 (El Niño periods) coincides with lower  $^{87}\text{Sr}/^{86}\text{Sr}$  value similar to that of average seawater value whereas higher  $^{87}\text{Sr}/^{86}\text{Sr}$  records were observed during the lower Niño 3.4 (La Niña) periods; they show significant inverse correlation ( $r = 0.49, n = 75, p < 0.01$ ). The vertical red bands represent El Niño periods and blue bands indicate La Niña interval. The coral  $^{87}\text{Sr}/^{86}\text{Sr}$  record is compared with (b) reconstructed salinity and (c) seasonal rainfall of Kerala (Rajeevan et al., 2008). GW and SW represent average groundwater and seawater  $^{87}\text{Sr}/^{86}\text{Sr}$  values. ML—Moderate La Niña, ME—Moderate El Niño, SE—Strong El Niño and SL—Strong La Niña.

$^{222}\text{Rn}$  (Jacob et al., 2009) and other coastal regions of the world 10–100 cm/day (Burnett et al., 2003 and references therein). Further, previous studies of Sr and  $^{87}\text{Sr}/^{86}\text{Sr}$  in groundwater of the Bengal basin (Basu Asish et al., 2001) and the Bay of Bengal (BOB) water column (Chakrabarti et al., 2018) have suggested that the BOB receives significant input of Sr via SGD, equivalent to its combined flux from the Ganga-Brahmaputra rivers. More recently, a comprehensive study (Damodararao

and Singh, 2022) on dissolved Sr and  $^{87}\text{Sr}/^{86}\text{Sr}$  was conducted in four major estuaries of the east coast of India such as the Ganga (Hooghly), Mahanadi, Godavari, and the Krishna and reported large supply of SGD to these estuaries. Based on Sr isotope mass balance, they have quantified SGD fluxes of  $\sim 11,000 \pm 900 \text{ m}^3 \text{s}^{-1}$  to these estuaries.

We observe more radiogenic values of  $^{87}\text{Sr}/^{86}\text{Sr}$  during the La Niña years characterised by stronger monsoon (Fig. 4a) and higher precipitation

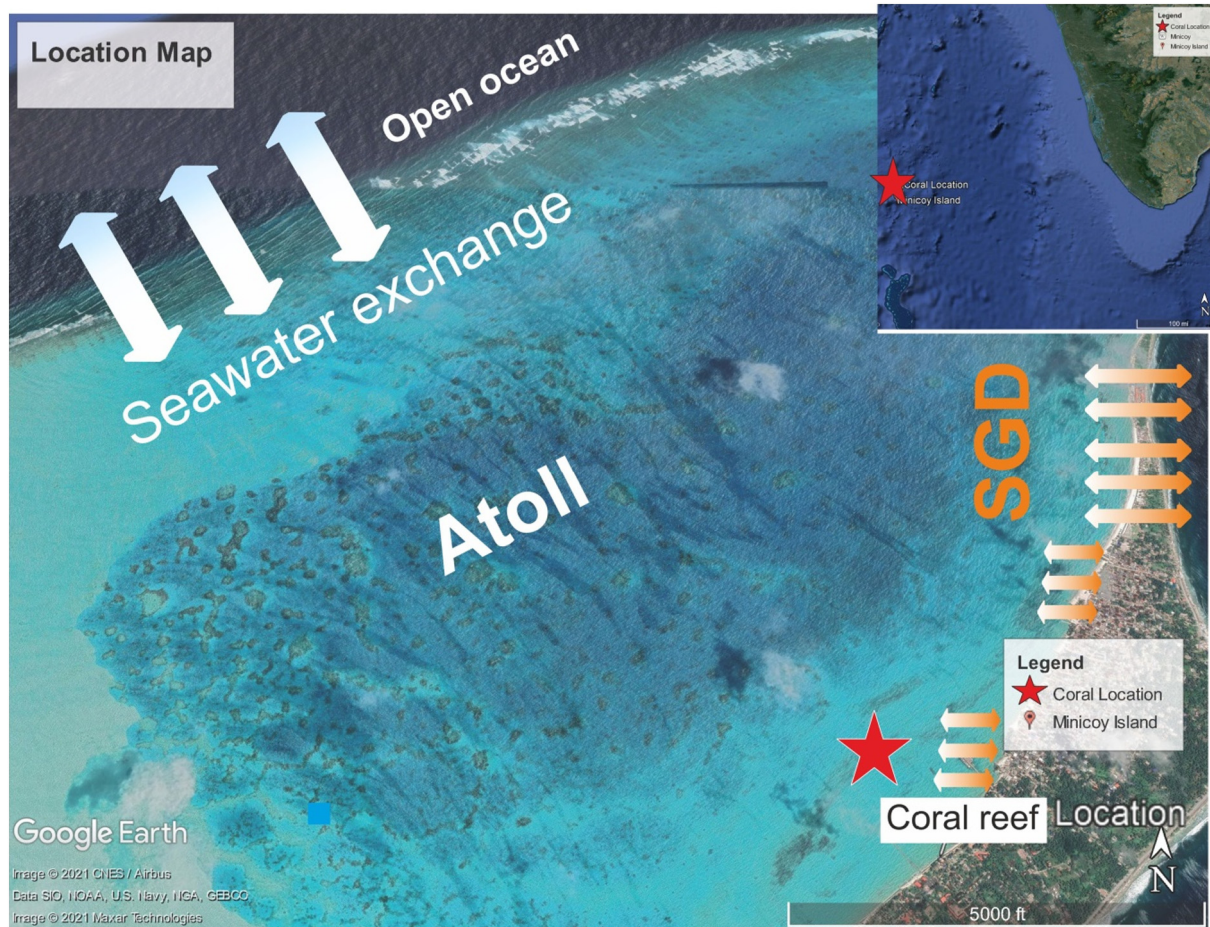


**Fig. 5.** Minicoy Atoll and coral reef location. White arrows indicate exchange of Atoll water with the open seawater. The orange colour arrows indicate submarine groundwater discharge (SGD) from the coastal aquifer. Red coloured star indicates coral location from where the sample was collected for the present study.

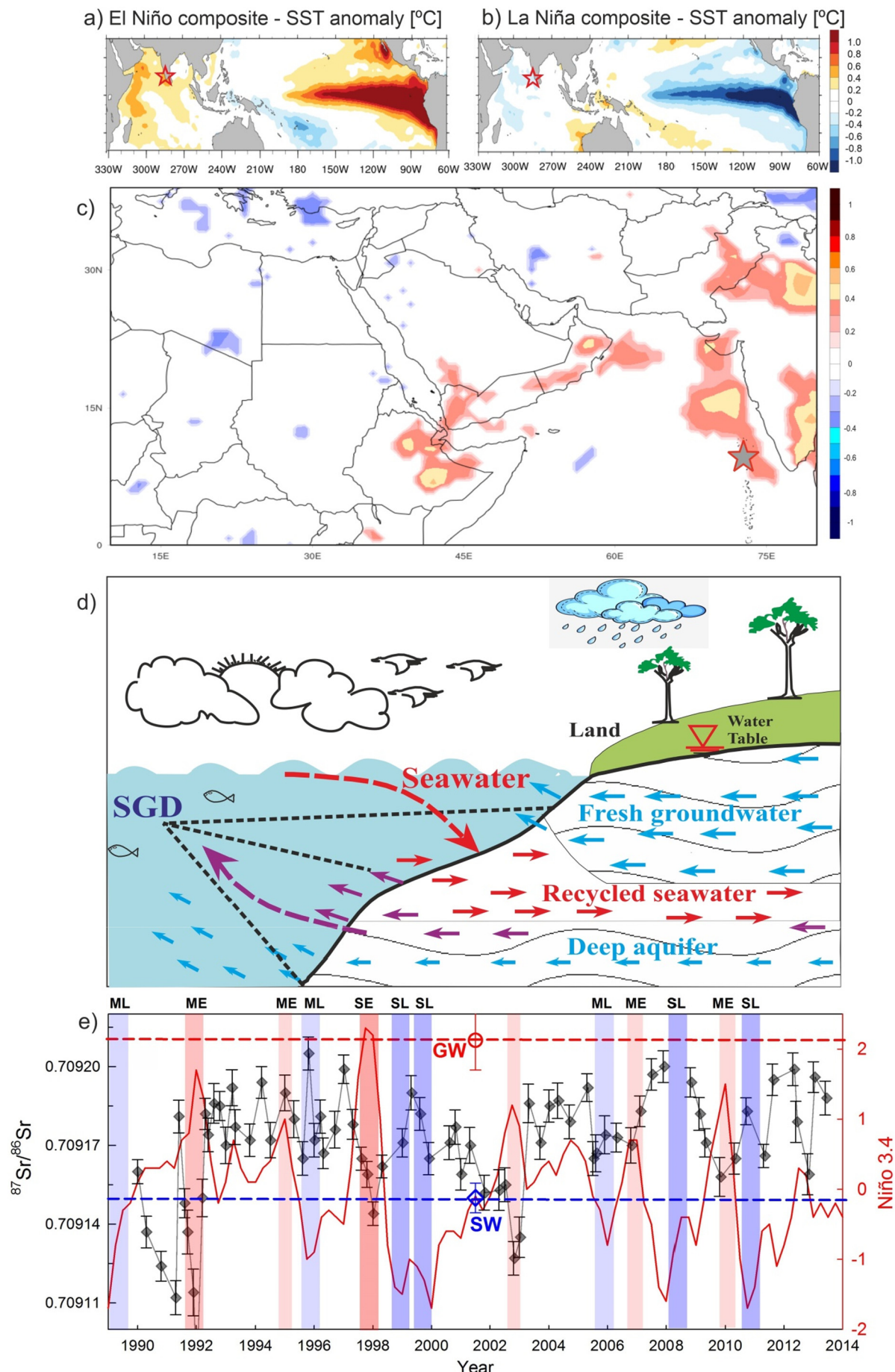
over India (Fig. 6c). Few groundwater samples ( $n = 3$ ) measured in the present study show significantly higher values ( $0.709206 \pm 0.000010$ ,  $2\sigma$ ) than the average Arabian sea water value ( $0.709150 \pm 0.000004$  ( $2\sigma$ )) (Rai, 2008). This indicates possible contribution of SGD to the Minicoy Atoll due to the higher monsoonal precipitation. Whereas, we observe lower  $^{87}\text{Sr}/^{86}\text{Sr}$  close to Arabian Sea water value during the El Niño years characterised by weaker monsoon and lower precipitation. This indicates minimum or negligible impact of SGD on the Minicoy Atoll. However, it is intriguing to observe slightly lower values than even the average Arabian Sea water during the El Niño years of 1991–92 (Fig. 4a). One of the possibilities could be more contribution of SGD (recycled component, Fig. 6c) that is derived from the chemical weathering of aquifer material comprised of Palaeozoic carbonates with lower  $^{87}\text{Sr}/^{86}\text{Sr}$  (Ca. 0.707 to 0.708) (Brand, 2004; Kani and Isozaki, 2021) and basaltic rocks similar to that of Lakshadweep and South-west Indian Ocean ridges Ca. 0.703 to 0.707 (Subha Anand et al., 2019). The occurrence of Palaeozoic carbonates has been reported from this region (Md and Vinayachandran, 2013). Groundwater in the Minicoy Island exists in the form of a thin freshwater lens over the saltwater, with restricted lateral movements. The mixing of seawater was found to be the predominant process controlling the configuration of freshwater lenses in these islands (Md and Vinayachandran, 2013), as reflected in the  $^{87}\text{Sr}/^{86}\text{Sr}$  and  $^{818}\text{O}$  records. A recent study to reconstruct pH record based on the boron isotope ( $\delta^{11}\text{B}$ ) of the same samples reveals large pH variability modulated by ENSO driven physical oceanographic processes (Tarique et al., 2021). Vertical mixing and upwelling modulated by ENSO events have been attributed to this large variability; lower pH during the El Niño and higher pH during the La Niña years. Groundwater is generally

characterised by lower pH than the average seawater ( $\text{pH}_{\text{sw}} \approx 8.1$ ) due to decomposition of organic matter in the aquifer. This low pH groundwater could be upwelled and/or vertically mixed with the surface water and lower the pH of the surface water (Correa et al., 2021; Lui et al., 2021). Therefore, observations in the earlier study also corroborate our conclusion in the present study and highlight the fact that the contribution of SGD must be taken into consideration while interpreting the Coral  $\delta^{11}\text{B}$ -pH record in similar settings elsewhere in the global oceans (Prouty et al., 2022).

#### 4.1. Quantitative estimates of past SGD fluxes modulated by ENSO

The SGD is defined as “any and all flow of water on continental margins” (Burnett et al., 2003; Moore, 2010b). This has primarily two components such as terrestrial fraction (“fresh SGD”) and the recycled component (“recycled SGD”) as illustrated in Fig. 6d. At global scale, recirculated seawater is estimated to be ~90 % of the total SGD whereas the fresh SGD only contributes to ~10 % of the total discharge volume (Kwon et al., 2014). Compared to rivers, fresh SGD supply accounts for 0.01–10 % of the water volume (Mackenzie and Garrels, 1971; Taniguchi et al., 2002). However, it is difficult to quantify separately these two components. In the present study, we have together treated them as SGD and hence any deviation from the average seawater  $^{87}\text{Sr}/^{86}\text{Sr}$  value could be accounted in terms of SGD Sr supply.

We have used the coral  $^{87}\text{Sr}/^{86}\text{Sr}$  record to generate semi-quantitative estimates of SGD fractions using Sr isotope mass balance for the entire



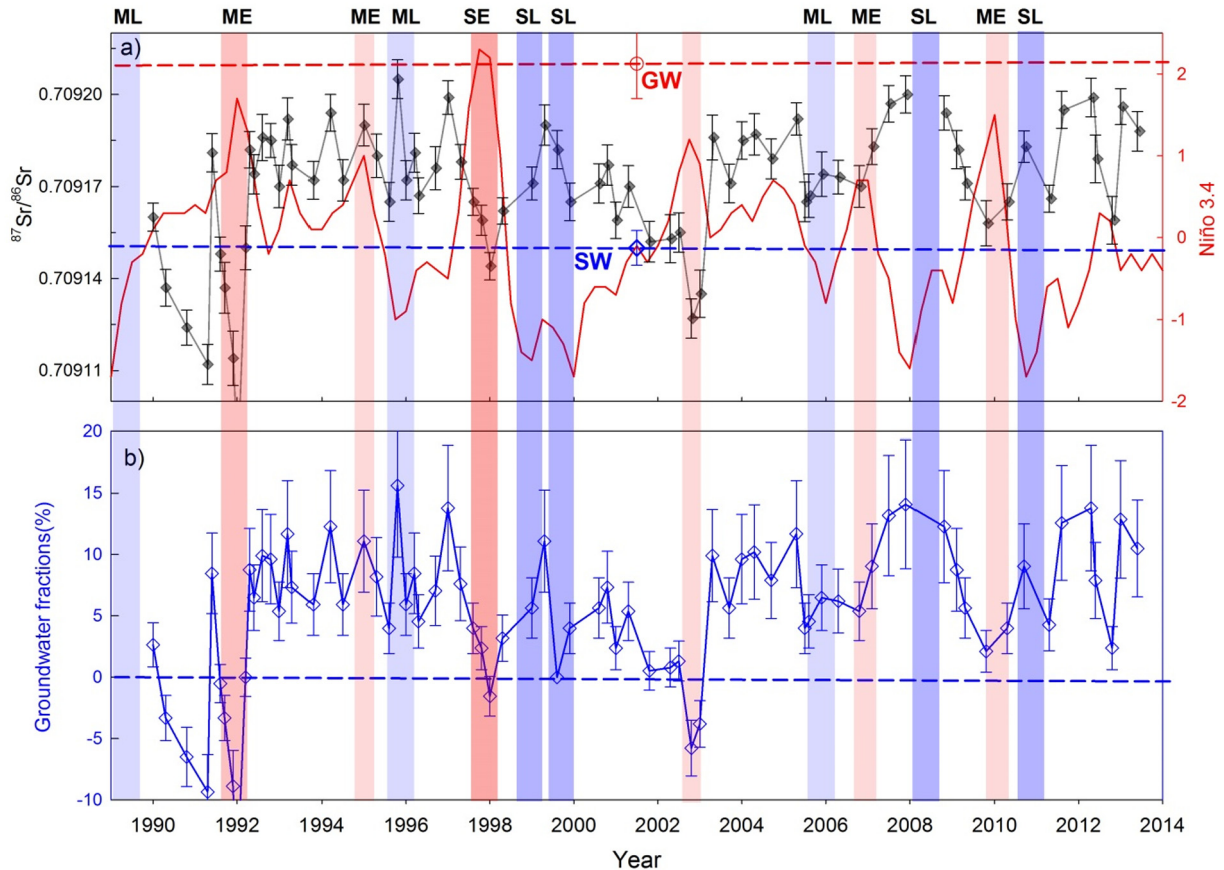


**Fig. 7.** (a) Coral  $^{87}\text{Sr}/^{86}\text{Sr}$  record is compared with Niño 3.4 index. (b) Record of submarine groundwater fractions corresponding to the  $^{87}\text{Sr}/^{86}\text{Sr}$  variations. The red bands indicate El Niño periods. ML—Moderate La Niña, ME—Moderate El Niño, SE—Strong El Niño and SL—Strong La Niña.

record (1990–2013). The SGD fractions were calculated using the binary mixing equation:

$$\left(\frac{^{87}\text{Sr}}{^{86}\text{Sr}}\right)_{\text{coral}} = \left(\frac{^{87}\text{Sr}}{^{86}\text{Sr}}\right)_{\text{SW}} \text{Sr}_{\text{SW}} \times f_{\text{SW}} + \left(\frac{^{87}\text{Sr}}{^{86}\text{Sr}}\right)_{\text{SGD}} \times \text{Sr}_{\text{SGD}} \times f_{\text{SGD}} \quad (1)$$

$$f_{\text{SW}} + f_{\text{SGD}} = 1 \quad (2)$$

where SW and SGD represent seawater and submarine groundwater endmembers whereas, Sr and f represent concentrations and fractions respectively. The underlying assumptions for these SGD fraction estimates are: (i) Sr isotope behaves conservatively, (ii) only two component mixing between seawater and SGD (i.e. binary mixing), and (iii) end-members of Sr concentration and  $^{87}\text{Sr}/^{86}\text{Sr}$  of seawater and SGD are accurately known. As discussed in earlier section, the  $^{87}\text{Sr}/^{86}\text{Sr}$  of the seawater endmember is taken to be the same as the reported value for the Arabian seawater  $0.709150 \pm 0.000004$  ( $2\sigma$ ) (Rai, 2008) with Sr concentration of  $\sim 90 \mu\text{mol/kg}$  ( $\sim 8 \text{ ppm}$ ) reported for open ocean waters (de Villiers, 1999; Palmer and Edmond, 1989) at salinity 35. The  $^{87}\text{Sr}/^{86}\text{Sr}$  value of the SGD endmember  $0.709210 \pm 0.000010$  ( $2\sigma$ ) was ascertained based

on three groundwater samples. The Sr concentration of the SGD was constrained based on the large data sets of the groundwater concentration is  $3.3 \pm 1.3 \text{ ppm}$  (Rahaman and Singh, 2012). The estimate of SGD fractions ranges from 0 to  $\sim 20 \%$ , minimum during the El Niño and maximum during the La Niña years (Fig. 7b). Our findings clearly highlight that the impact of the past ENSO events on coastal hydrology can be traced and quantitatively assessed using coral  $^{87}\text{Sr}/^{86}\text{Sr}$  record.

#### 4.2. Implications

Submarine groundwater discharge has been recognized as an important pathway through which nutrients and chemical fluxes are supplied to oceans (Burnett et al., 2006; Moosdorf and Oehler, 2017). Based on our key finding of ENSO-SGD relationship in the present study and model predictions of future increase in ENSO event frequency and amplitude (Cai et al., 2014; Oliver et al., 2018), we expect large variability in chemical and nutrient fluxes to coastal oceans supplied by SGD. These ENSO driven future changes in SGD can impact coastal environments (e.g. Eh, pH, salinity, temperature) and cause a potential threat to the extremely sensitive coral ecosystem and other marine organisms.

**Fig. 6.** Schematics showing the influence of El Niño–Southern Oscillation on SGD variability. Correlation between June–July–August sea surface temperature anomalies during (a) El Niño years and (b) La Niña years. Colour bar represents correlation coefficients significant at the 99 % confidence level. The open star represents coral location. (c) Spatial correlation of ERA-5 reanalysis precipitation record (1979–2019, June–July–August) with SOI record. The regions of significant spatial correlations (at 90 % significance level) are highlighted in colour band. Spatial correlation is plotted using online climate analyzer software ([http://cci-reanalyzer.org/reanalysis/monthly\\_correl/](http://cci-reanalyzer.org/reanalysis/monthly_correl/)). Red star indicates location of the Lakshadweep coral reef. (d) Schematic of submarine groundwater discharge into coastal regions. Arrows indicate water flow directions. (e) Coral  $^{87}\text{Sr}/^{86}\text{Sr}$  record is plotted with Nino 3.4 record. The red and blue colour bands indicate El Niño and La Niña events respectively. ML—Moderate La Niña, ME—Moderate El Niño, SE—Strong El Niño and SL—Strong La Niña. SW and GW represent average seawater and groundwater  $^{87}\text{Sr}/^{86}\text{Sr}$  values respectively.

The key finding of the present study highlights that coral  $^{87}\text{Sr}/^{86}\text{Sr}$  record could be a potential proxy for quantifying past changes in the SGD fluxes and inferring about past hydro-climatic changes impacted by ENSO events. The pre-requisite to use coral  $^{87}\text{Sr}/^{86}\text{Sr}$  as a proxy for SGD includes (i) Sr isotopes behave conservatively, (ii) mixing component end-members of Sr concentration and  $^{87}\text{Sr}/^{86}\text{Sr}$  of seawater and SGD are accurately known and (iii) coral  $^{87}\text{Sr}/^{86}\text{Sr}$  variations are resolvable within the analytical uncertainty. However, more coral  $^{87}\text{Sr}/^{86}\text{Sr}$  records need to be obtained from other atolls with diverse oceanographic settings and climatic regimes to test the potential of this proxy more rigorously. In addition, some of the important aspects of any novel proxy such as sensitivity, uncertainty and caveats attached with its application need to be assessed with large number of coral  $^{87}\text{Sr}/^{86}\text{Sr}$  records. For example, though present study has demonstrated that the Lakshadweep coral  $^{87}\text{Sr}/^{86}\text{Sr}$  record captured most of the ENSO events throughout the record, however, the amplitude of their excursions does not correspond well to the amplitude of each ENSO events and also the  $^{87}\text{Sr}/^{86}\text{Sr}$ -El Niño 3.4 relationship breaks in some of the intervals (Fig. 5). At this stage, we could not unequivocally conclude whether it is related to the sensitivity of the coral  $^{87}\text{Sr}/^{86}\text{Sr}$  to the ENSO induced SGD changes or lead-lag between ENSO induced precipitation changes and its impact on SGD reservoirs. However, with this sensitivity of proxy observed in the present study, the high-resolution long records of coral  $^{87}\text{Sr}/^{86}\text{Sr}$  from the Lakshadweep and elsewhere will definitely give an immense opportunity to reconstruct longer ENSO records and to assess the hydrological and hydro-climatic impact over more spatial extent in a long-term perspective.

## 5. Conclusions

The Sr isotope record of Lakshadweep coral shows resolvable variations and good correspondence with the past ENSO events; more radiogenic values of  $^{87}\text{Sr}/^{86}\text{Sr}$  coincide with the La Niña years and less radiogenic values with El Niño years. Our investigation reveals significant supply of more radiogenic Sr via SGD to the Minicoy Atoll during the La Niña years whereas minimum or negligible supply of radiogenic Sr during the El Niño years. Based on Sr isotope mass balance, we have estimated SGD fractions supplied to the Minicoy Atoll for the entire record range from 0 to ~20 % with minimum during the El Niño years and maximum during the La Niña years. Our key finding of  $^{87}\text{Sr}/^{86}\text{Sr}$ -ENSO relationship through the changes in SGD induced by precipitation changes highlights the potential application of coral  $^{87}\text{Sr}/^{86}\text{Sr}$  as a proxy for the reconstruction of past ENSO events and tracing its impact on regional hydrology and hydroclimate. Numerical models have predicted increasing frequency and amplitude of ENSO events (Cai et al., 2014; Collins et al., 2010) and therefore, ENSO driven large variability in SGD supply may severely impact coastal environments (e.g. Eh, pH, salinity, temperature) and biogeochemical processes.

## CRediT authorship contribution statement

Walir Rahaman and Mohd Tarique designed the study. Walir Rahaman wrote the first draft. Mohd Tarique and Priyesh Prabhat analysed the samples. Fausiya A.A. and Hema Achyuthan provided the coral sample. All authors contributed to interpreting results, discussion and improvement of this paper.

**Conceptualization:** Walir Rahaman, Mohd Tarique

**Methodology:** Walir Rahaman, Mohd Tarique

**Validation:** Walir Rahaman, Mohd Tarique

**Formal analysis:** Walir Rahaman

**Investigation:** Mohd Tarique, Priyesh Prabhat

**Data Curation:** Mohd Tarique, Priyesh Prabhat

**Resources:** A. A. Fausiya, Hema Achyuthan

**Supervision:** Walir Rahaman

**Writing – original draft:** Walir Rahaman

**Writing – review & editing:** Walir Rahaman, Mohd Tarique, A. A. Fausiya, Priyesh Prabhat, Hema Achyuthan

## Declaration of competing interest

The authors declare no competing interests.

## Acknowledgments

We acknowledge the National Centre for Polar and Ocean, Goa, Ministry of Earth Sciences, India for financial support through the project “PACER - Cryosphere and Climate”. We are grateful to director NCPO, M. Ravichandran for his continuous support and encouragement. Authors also acknowledge UGC for the NET/JRF fellowship to Mohd Tarique. This is the NCPO contribution number J-23/2022-23.

## Appendix A. Supplementary data

Supplementary data to this article can be found online at <https://doi.org/10.1016/j.scitotenv.2022.157035>.

## References

- Aalto, R., Maurice-Bourgois, L., Dunne, T., Montgomery, D.R., Nittrouer, C.A., Guyot, J.-L., 2003. Episodic sediment accumulation on amazonian flood plains influenced by El Niño/Southern oscillation. *Nature* 425, 493–497.
- Achyuthan, H., Deshpande, R.D., Rao, M.S., Kumar, B., Nallathambi, T., Shashi Kumar, K., Ramesh, R., Ramachandran, P., Maurya, A.S., Gupta, S.K., 2013. Stable isotopes and salinity in the surface waters of the bay of Bengal: implications for water dynamics and palaeoclimate. *Mar. Chem.* 149, 51–62.
- Ahmad, S.M., Padmakumari, V.M., Raza, W., Venkatesham, K., Suseela, G., Sagar, N., Chamoli, A., Rajan, R.S., 2011. High-resolution carbon and oxygen isotope records from a scleractinian (*Porites*) coral of Lakshadweep archipelago. *Quat. Int.* 238, 107–114.
- Azad, S., Rajeevan, M., 2016. Possible shift in the ENSO-indian monsoon rainfall relationship under future global warming. *Sci. Rep.* 6, 20145.
- Barker, S., Greaves, M., Elderfield, H., 2003. A study of cleaning procedures used for foraminiferal Mg/Ca paleothermometry. *Geochim., Geophys., Geosyst.* 4, 8407.
- Basu Asish, R., Jacobsen Stein, B., Poreda Robert, J., Dowling Carolyn, B., Aggarwal Pradeep, K., 2001. Large groundwater strontium flux to the oceans from the Bengal Basin and the marine strontium isotope record. *Science* 293, 1470–1473.
- Behara, A., Vinayachandran, P.N., Shankar, D., 2019. Influence of rainfall over eastern Arabian Sea on its salinity. *J. Geophys. Res. Oceans* 124, 5003–5020.
- Boyer, T., Baranova, O., Locarnini, R., Mishonov, A., Grodsky, A., Paver, C., Weathers, K., Smolyar, I., Reagan, J., Seidov, D., Zweng, M., 2019. WORLD OCEAN ATLAS 2018 Product Documentation Ocean Climate Laboratory NCEI / NESDIS / NOAA NOAA National Centers for Environmental Information.
- Braganza, K., Gergis, J.L., Power, S.B., Risbey, J.S., Fowler, A.M., 2009. A multiproxy index of the El Niño-Southern Oscillation, A.D. 1525–1982. *J. Geophys. Res. Atmos.* 114, D05106.
- Brand, U., 2004. Carbon, oxygen and strontium isotopes in paleozoic carbonate components: an evaluation of original seawater-chemistry proxies. *Chem. Geol.* 204, 23–44.
- Burnett, W., Bokuniewicz, H., Huettel, M., Moore, W., Taniguchi, M., 2003. Groundwater and pore water inputs to the coastal zone. *Biogeochemistry* 66, 3–33.
- Burnett, W.C., Aggarwal, P.K., Aureli, A., Bokuniewicz, H., Cable, J.E., Charette, M.A., Kontar, E., Krupa, S., Kulkarni, K.M., Loveless, A., Moore, W.S., Oberdorfer, J.A., Oliveira, J., Ozuyurt, N., Povinec, P., Privitera, A.M.G., Rajar, R., Ramessur, R.T., Scholten, J., Stieglitz, T., Taniguchi, M., Turner, J.V., 2006. Quantifying submarine groundwater discharge in the coastal zone via multiple methods. *Sci. Total Environ.* 367, 498–543.
- Cai, W., Borlace, S., Lengaigne, M., van Rensh, P., Collins, M., Vecchi, G., Timmermann, A., Santoso, A., McPhaden, M.J., Wu, L., England, M.H., Wang, G., Guleyardi, E., Jin, F.-F., 2014. Increasing frequency of extreme El Niño events due to greenhouse warming. *Nat. Clim. Cha.* 4, 111–116.
- Chakrabarti, R., Mondal, S., Acharya, S.S., Lekha, J.S., Sengupta, D., 2018. Submarine groundwater discharge derived strontium from the Bengal Basin traced in bay of Bengal water samples. *Sci. Rep.* 8, 4383.
- Chakraborty, S., Ramesh, R., 1993. Monsoon-Induced Sea surface temperature changes recorded in Indian corals. *Terra Nova* 5, 545–551.
- Chakraborty, S., Goswami, B.N., Dutta, K., 2012. Pacific coral oxygen isotope and the tropospheric temperature gradient over the Asian monsoon region: a tool to reconstruct past Indian summer monsoon rainfall. *J. Quat. Sci.* 27, 269–278.
- Chatterjee, J., Singh, S.K., 2012.  $^{87}\text{Sr}/^{86}\text{Sr}$  and major ion composition of rainwater of Ahmedabad, India: sources of base cations. *Atmos. Environ.* 63, 60–67.
- Collins, M., An, S.-J., Cai, W., Ganachaud, A., Guiyadi, E., Jin, F.-F., Jochum, M., Lengaigne, M., Power, S., Timmermann, A., Vecchi, G., Wittenberg, A., 2010. The impact of global warming on the tropical Pacific Ocean and El Niño. *Nat. Geosci.* 3, 391.
- Consortium, P.A.K., 2017. A global multiproxy database for temperature reconstructions of the Common Era. *Scientific Data* 4, 170088.
- Correa, R.E., Cardenas, M.B., Rodolfo, R.S., Lapus, M.R., Davis, K.L., Giles, A.B., Fullon, J.C., Hajati, M.-C., Moosdorf, N., Sanders, C.J., Santos, I.R., 2021. Submarine groundwater discharge releases CO<sub>2</sub> to a coral reef. *ACS EST Water* 1, 1756–1764.
- Correge, T., 2006. Sea surface temperature and salinity reconstruction from coral geochemical tracers. *Palaeoceanogr., palaeocliPalaeoec.* 232, 408–428.

- Corrège, T., 2006. Sea surface temperature and salinity reconstruction from coral geochemical tracers. *Palaeogeogr. Palaeoclimatol. Palaeoecol.* 232, 408–428.
- D'Arrigo, R., Wilson, R., Deser, C., Wiles, G., Cook, E., Villalba, R., Tudhope, A., Cole, J., Linsley, B., 2005. Tropical-North Pacific climate linkages over the past four centuries. *J. Clim.* 18, 5253–5265.
- Damodararao, K., Singh, S.K., 2022. Substantial submarine groundwater discharge in the estuaries of the east coast of India and its impact on marine strontium budget. *Geochim. Cosmochim. Acta* 324, 66–85.
- Danish, M., Tripathy, G.R., Rahaman, W., 2020. Submarine groundwater discharge to a tropical coastal lagoon (Chilika lagoon, India): an estimation using Sr isotopes. *Mar. Chem.* 224, 103816.
- Dansgaard, W., 1964. Stable isotopes in precipitation. *Tellus* 16, 436–468.
- de Villiers, S., 1999. Seawater strontium and Sr/Ca variability in the Atlantic and Pacific oceans. *EPSL* 171, 623–634.
- DeLong, K.L., Quinn, T.M., Taylor, F.W., 2007. Reconstructing twentieth-century sea surface temperature variability in the Southwest Pacific: a replication study using multiple coral Sr/Ca records from New Caledonia. *Paleoceanography* 22, PA4212.
- DeLong, K.L., Quinn, T.M., Taylor, F.W., Shen, C.-C., Lin, K., 2013. Improving coral-base paleoclimate reconstructions by replicating 350 years of coral Sr/Ca variations. *Palaeogeogr. Palaeoclimatol. Palaeoecol.* 373, 6–24.
- Fan, T., Yu, K., Zhao, J., Jiang, W., Xu, S., Zhang, Y., Wang, R., Wang, Y., Feng, Y., Bian, L., Qian, H., Liao, W., 2019. Strontium isotope stratigraphy and paleomagnetic age constraints on the evolution history of coral reef islands, northern South China Sea. *GSAT Bull.* 132, 803–816.
- Fietzke, J., Eisenhauer, A., 2006. Determination of temperature-dependent stable strontium isotope ( $^{88}\text{Sr}/^{86}\text{Sr}$ ) fractionation via bracketing standard MC-ICP-MS. *Geochem., Geophys., Geosyst.* 7, Q08009.
- Fousiya, A.A., Chakraborty, S., Achyuthan, H., Gandhi, N., Sinha, N., Datye, A., 2016. Stable isotopic investigation of Porites coral from the Minicoy Island. *Indian J. Geo Mar. Sci.* 45, 1465–1470.
- Fowell, S.E., Sandford, K., Stewart, J.A., Castillo, K.D., Ries, J.B., Foster, G.L., 2016. Intrareef variations in Li/Mg and Sr/Ca sea surface temperature proxies in the Caribbean reef-building coral *Siderastrea siderea*. *Paleoceanography* 31, 1315–1329.
- Fowler, A.M., Boswijk, G., Lorrey, A.M., Gergis, J., Pirie, M., McCloskey, S.P.J., Palmer, J.G., Wunder, J., 2012. Multi-centennial tree-ring record of ENSO-related activity in New Zealand. *Nat. Clim. Chang.* 2, 172.
- Gagan, M., Ayliffe, L., Hopley, D., Cali, J., Mortimer, G., Chappell, J., McCulloch, M., Head, M., 1998. Temperature and Surface-Ocean water balance of the mid-holocene tropical Western Pacific. *Science (New York, N.Y.)* 279, 1014–1018.
- Hendy, E.J., Gagan, M.K., Alibert, C.A., McCulloch, M.T., Lough, J.M., Isdale, P.J., 2002. Abrupt decrease in tropical Pacific Sea surface salinity at end of little ice age. *Science* 295, 1511–1514.
- Huang, K.F., You, C.F., Chung, C.H., Lin, I.T., 2011. Nonhomogeneous seawater Sr isotopic composition in the coastal oceans: A novel tool for tracing water masses and submarine groundwater discharge. *Geochem., Geophys., Geosyst.* 12, Q5002.
- Jacob, N., Babu, D.S., Shivanna, K., 2009. Radon as an indicator of submarine groundwater discharge in coastal regions. *Curr. Sci.* 1313–1320.
- Johannesson, K.H., Chevis, D.A., Burdige, D.J., Cable, J.E., Martin, J.B., Roy, M., 2011. Submarine groundwater discharge is an important net source of light and middle REEs to coastal waters of the Indian River lagoon, Florida, USA. *Geochim. Cosmochim. Acta* 75, 825–843.
- Kalnay, E., Kanamitsu, M., Kistler, R., Collins, W., Deaven, D., Gandin, L., Iredell, M., Saha, S., White, G., Woollen, J., Zhu, Y., Chelliah, M., Ebisuzaki, W., Higgins, W., Janowiak, J., Mo, K.C., Ropelewski, C., Wang, J., Leetmaa, A., Reynolds, R., Jenne, R., Joseph, D., 1996. The NCEP/NCAR 40-year reanalysis project. *Bull. Am. Meteorol. Soc.* 77, 437–472.
- Kani, T., Isozaki, Y., 2021. The capitanian minimum: a unique sr isotope Beacon of the latest paleozoic seawater. *Frontiers in Earth Science* 9.
- Kripalani, R., Kulkarni, A., 1997. Climatic impact of El Niño/La Niña on the Indian monsoon: a new perspective. *Weather* 52, 39–46.
- Kwon, E.Y., Kim, G., Primeau, F., Moore, W.S., Cho, H.-M., DeVries, T., Sarmiento, J.L., Charette, M.A., Cho, Y.-K., 2014. Global estimate of submarine groundwater discharge based on an observationally constrained radium isotope model. *Geophys. Res. Lett.* 41, 8438–8444.
- Leupold, M., Pfeiffer, M., Watanabe, T.K., Reuning, L., Garbe-Schönberg, D., Shen, C.C., Brummer, G.J.A., 2021. El Niño-southern oscillation and internal sea surface temperature variability in the tropical Indian Ocean since 1675. *Clim. Past* 17, 151–170.
- Liu, G., Kojima, K., Yoshimura, K., Oka, A., 2014. Proxy interpretation of coral-recorded seawater  $\delta^{18}\text{O}$  using 1-D model forced by isotope-incorporated GCM in tropical oceanic regions. *J. Geophys. Res.-Atmos.* 119, 12,021–012,033.
- Liu, Y.W., Aceijo, S.M., Wanamaker Jr., A.D., 2015. Environmental controls on the boron and strontium isotopic composition of aragonite shell material of cultured *Arctica islandica*. *Biogeosciences* 12, 3351–3368.
- Liu, H.-K., Liu, M.-Y., Lin, H.-C., Tseng, H.-C., Liu, L.-L., Wang, F.-Y., Hou, W.-P., Chang, R., Chen, C.-T.A., 2021. Hydrogeochemistry and Acidic Property of Submarine Groundwater Discharge Around Two Coral Islands in the Northern South China Sea. 9.
- Mackenzie, F., Garrels, R., 1971. Evolution of Sedimentary Rocks: New York.
- Mallik, T., 2017. Coral atolls of Lakshadweep, Arabian Sea, Indian Ocean. *MOJ Ecology & Environmental Sciences* 2 (2), 68–83.
- McCulloch, M.T., Gagan, M.K., Mortimer, G.E., Chivas, A.R., Isdale, P.J., 1994. A high-resolution Sr/Ca and  $\delta^{18}\text{O}$  coral record from the great barrier reef, Australia, and the 1982–1983 El Niño. *Geochim. Cosmochim. Acta* 58, 2747–2754.
- Md, N.K., Vinayachandran, N., 2013. Chemical evolution of groundwater in the coral islands of Lakshadweep archipelago, India with special reference to Kavaratti island. *Nat. Environ. Pollut. Technol.* 12, 43–50.
- Moore, W.S., 2010a. The effect of submarine groundwater discharge on the ocean. *Annu. Rev. Mar. Sci.* 2, 59–88.
- Moore, W.S., 2010b. Submarine groundwater discharge. *Encyclopedia of Ocean Sciences*, pp. 551–558.
- Moosdorf, N., Oehler, T., 2017. Societal use of fresh submarine groundwater discharge: an overlooked water resource. *Earth Sci. Rev.* 171, 338–348.
- Moquet, J.-S., Morera, S., Turcq, B., Poitrasson, F., Roddaz, M., Moreira-Turcq, P., Espinoza, J.C., Guyot, J.-L., Takahashi, K., Orrillo-Vigo, J., Petrick, S., Mounic, S., Sondag, F., 2020. Control of seasonal and inter-annual rainfall distribution on the strontium-neodymium isotopic compositions of suspended particulate matter and implications for tracing ENSO events in the Pacific coast (Tumbes basin, Peru). *Glob. Planet. Chang.* 185, 103080.
- Nuruzzama, M., Rahaman, W., Tripathy, G.R., Mohan, R., Patil, S., 2020. Dissolved major ions, Sr and  $^{87}\text{Sr}/^{86}\text{Sr}$  of coastal lakes from Larsemann hills, East Antarctica: Solute sources and chemical weathering in a polar environment. *Hydrol. Process.* 34, 2351–2364.
- Oliver, E.C.J., Donat, M.G., Burrows, M.T., Moore, P.J., Smale, D.A., Alexander, L.V., Benthuysen, J.A., Feng, M., Sen Gupta, A., Hobday, A.J., Holbrook, N.J., Perkins-Kirkpatrick, S.E., Scannell, H.A., Straub, S.C., Wernberg, T., 2018. Longer and more frequent marine heatwaves over the past century. *Nat. Commun.* 9, 1324.
- Palmer, M.R., Edmond, J.M., 1989. The strontium isotope budget of the modern ocean. *EPSL* 92, 11–26.
- Pfeiffer, M., Dullo, W.-C., Zinke, J., Garbe-Schönberg, D., 2009. Three monthly coral Sr/Ca records from the chagos archipelago covering the period of 1950–1995 a.D.: reproducibility and implications for quantitative reconstructions of sea surface temperature variations. *Int. J. Earth Sci.* 98, 53–66.
- Pfeiffer, M., Reuning, L., Zinke, J., Garbe-Schönberg, D., Leupold, M., Dullo, W.C., 2019. 20th century  $\delta^{18}\text{O}$  seawater and salinity variations reconstructed from paired  $\delta^{18}\text{O}$  and Sr/Ca measurements of a La Reunion Coral. *Paleoceanogr. and Paleoclimatol.* 34, 2183–2200.
- Pillai, C.S., 1971. The distribution of shallow-water stony corals at minicoy atoll in the Indian Ocean; with a check-list of species. *Atoll Res. Bull.* 141, 1–12.
- Pin, C., Bassin, C., 1992. Evaluation of a strontium-specific extraction chromatographic method for isotopic analysis in geological materials. *Anal. Chim. Acta* 269, 249–255.
- Prouty, N.G., Wall, M., Fietzke, J., Cheriton, O.M., Anagnostou, E., Phillips, B.L., Paytan, A., 2022. The role of pH up-regulation in response to nutrient-enriched, low-pH groundwater discharge. *Mar. Chem.* 243, 104134.
- Raddatz, J., Liebetrau, V., Rüggeberg, A., Hathorne, E., Krabbenhoft, A., Eisenhauer, A., Böhm, F., Vollstaedt, H., Fietzke, J., López Correa, M., Freiwald, A., Dullo, W.C., 2013. Stable Sr-isotope, Sr/Ca, Mg/Ca, Li/Ca and Mg/Li ratios in the scleractinian cold-water coral *Lophelia Pertusa*. *Chem. Geol.* 352, 143–152.
- Rahaman, W., Singh, S.K., 2012. Sr and  $^{87}\text{Sr}/^{86}\text{Sr}$  in estuaries of western India: impact of submarine groundwater discharge. *Geochim. Cosmochim. Acta* 85, 275–288.
- Rahaman, W., Singh, S.K., Sinha, R., Tandon, S.K., 2011. Sr, C and O isotopes in carbonate nodules from the Ganga plain: evidence for recent abrupt rise in dissolved  $^{87}\text{Sr}/^{86}\text{Sr}$  ratios of the Ganga. *Chem. Geo.* 285, 184–193.
- Rahaman, W., Chatterjee, S., Ejaz, T., Thamban, M., 2019. Increased influence of ENSO on Antarctic temperature since the industrial era. *Sci. Rep.* 9, 6006.
- Rai, S.K., 2008. Isotopic and Geochemical Studies of Ancient and Modern Sediments. Ph. D. ThesisMS University, Vadodara 195 pp.
- Rajeevan, M., Pal, D.S., 2007. On the El Niño-indian monsoon predictive relationships. *Geophys. Res. Lett.* 34, L04704.
- Rajeevan, M., Bhate, J., Jaswal, A.K., 2008. Analysis of variability and trends of extreme rainfall events over India using 104 years of gridded daily rainfall data. *Geophys. Res. Lett.* 35.
- Rüggeberg, A., Fietzke, J., Liebetrau, V., Eisenhauer, A., Dullo, W.-C., Freiwald, A., 2008. Stable strontium isotopes (88Sr/86Sr) in cold-water corals — a new proxy for reconstruction of intermediate ocean water temperatures. *Earth Planet. Sci. Lett.* 269, 570–575.
- Sadler, J., Webb, G.E., Nothdurft, L.D., Dechnik, B., 2014. Geochemistry-based coral paleoclimate studies and the potential of 'non-traditional' (non-massive Porites) corals: recent developments and future progression. *Earth Sci. Rev.* 139, 291–316.
- Sagar, N., Hetzinger, S., Pfeiffer, M., Ahmad, S., Dullo, W.-C., Garbe-Schönberg, D., 2015. High-resolution Sr/Ca ratios in a *Porites lutea* coral from Lakshadweep archipelago, southeast Arabian Sea: an example from a region experiencing steady rise in the reef temperature. *J. Geophys. Res. Oceans* 121, 252–266.
- Sagar, N., Hetzinger, S., Pfeiffer, M., Masood Ahmad, S., Dullo, W.-C., Garbe-Schönberg, D., 2016. High-resolution Sr/Ca ratios in a *Porites lutea* coral from Lakshadweep archipelago, southeast Arabian Sea: an example from a region experiencing steady rise in the reef temperature. *J. Geophys. Res. Oceans* 121, 252–266.
- Schott, F.A., Xie, S.-P., McCreary Jr., J.P., 2009. Indian Ocean circulation and climate variability. *Rev. Geophys.* 47.
- Shankar, D., Vinayachandran, P.N., Unnikrishnan, A.S., 2002. The monsoon currents in the North Indian Ocean. *Prog. Oceanog.* 52, 63–120.
- Shen, C.-C., Lee, T., Liu, K.-K., Hsu, H.-H., Edwards, R., Wang, C.-H., Lee, M.-Y., Chen, Y.-G., Lee, H.-J., Sun, H.-T., 2005. An evaluation of quantitative reconstruction of past precipitation records using coral skeletal Sr/Ca and  $\delta^{18}\text{O}$  data. *EPSL* 237, 370–386.
- Singh, A., Jani, R., Ramesh, R., 2010. Spatiotemporal variations of the  $\delta^{18}\text{O}$ -salinity relation in the northern Indian Ocean. *Deep-Sea Res. I Oceanogr. Res. Pap.* 57, 1422–1431.
- Subha Anand, S., Rahaman, W., Lathika, N., Thamban, M., Patil, S., Mohan, R., 2019. Trace elements and Sr, Nd isotope compositions of surface sediments in the Indian Ocean: an evaluation of sources and processes for sediment transport and dispersal. *Geochim. Geophys. Geosyst.* 20, 3090–3112.
- Taniguchi, M., Burnett, W.C., Cable, J.E., Turner, J.V., 2002. Investigation of submarine groundwater discharge. *Hydrol. Process.* 16, 2115–2129.
- Tarique, M., Rahaman, W., Fousiya, A.A., Lathika, N., Thamban, M., Achyuthan, H., Misra, S., 2021. Surface pH record (1990–2013) of the Arabian sea from boron isotopes of Lakshadweep corals—trend, variability, and control. *Journal of Geophysical Research: Biogeosciences* 126, e2020JG006122.

- Thompson, D.M., 2022. Environmental records from coral skeletons: a decade of novel insights and innovation. *WIREs Clim. Change* 13, e745.
- Wakaki, S., Obata, H., Tazoe, H., Ishikawa, T., 2017. Precise and accurate analysis of deep and surface seawater  $\text{Sr}$  stable isotopic composition by double-spike thermal ionization mass spectrometry. *Geochem. J.* 51, 227–239.
- Wei, Y., Deng, W., Ma, J., Chen, X., Zeng, T., Wei, G., 2022. Evaluation of coral skeletal  $88\text{Sr}$  as a paleoclimate proxy in the northern South China Sea. *Palaeogeogr. Palaeoclimatol. Palaeoecol.* 592, 110906.
- Weis, D., Kieffer, B., Maerschalk, C., Barling, J., De Jong, J., Williams, G., Hanano, D., Pretorius, W., Mattielli, N., Scoates, J., Goolaerts, A., Friedman, R., Mahoney, J., 2006. High-precision isotopic characterization of USGS reference materials by TIMS and MC-ICP-MS. *Geochem. Geophys. Geosyst.* 7, Q08006.
- Wilkinson, C., 2000. *Status of Coral Reefs of the World: 2000*. Australian Institute of Marine Science.
- Zinke, J., Rühs, S., Pfeiffer, M., Watanabe, T.K., Grab, S., Garbe-Schönberg, D., Biastoch, A., 2021. 334-year coral record of surface temperature and salinity variability in the greater Agulhas current region. *Clim. Past Discuss.* 2021, 1–30.